Available online at www.sciencedirect.com
SCIENCE DIRECT®
Journal of Sound and Vibration 294 (2006) 397–409
JOURNAL OF SOUND AND VIBRATION
www.elsevier.com/locate/jsvi

Short Communication

Time–frequency distributions for crack detection in rotors—A fundamental note

Khoa N. Le*

School of Engineering, Griffith University, Gold Coast Campus, QLD 4215, Australia

Received 16 February 2005; received in revised form 27 October 2005; accepted 14 November 2005
Available online 4 January 2006

Abstract

This correspondence gives insight into properties of Wigner–Ville time–frequency power spectral analysis and also suggests better time–frequency power spectral tools to study cracks in rotors. Simulation results show that Choi–Williams and hyperbolic distributions can be effectively used for crack detection in rotors.

1. Motivation

This work is initiated by the work of Zou and Chen [1] in which Wigner–Ville (WV) time–frequency distribution was successfully used for crack detection in rotors. The aims of this correspondence are three-fold: (1) providing insight into WV time–frequency power spectrum and its major fundamental drawbacks; (2) suggesting more effective time–frequency distributions, such as Choi–Williams (CW) and hyperbolic (Hy), for crack detection in rotors; and (3) highlighting a close relationship between kernels and symmetrical wavelets.

The paper is organised as follows. Section 2 gives background on time–frequency distributions and popular kernels which have been reported in the literature. Section 3 identifies important drawbacks of WV time–frequency distribution. Section 4 briefly introduces new symmetrical Hy and CW wavelets, and stating the relationship between time–frequency kernels and wavelets. Section 5.1 graphically illustrates the drawback of WV time–frequency distribution by using CW and Hy distributions. Section 5.2 shows that these time–frequency distributions can be effectively used for crack detection. Section 6 concludes the main findings of the paper and also outlines further work.

2. Background on time–frequency power spectrum

Time–frequency signal processing has progressed to a stable and mature field with many works and contributions reported in Refs. [2–7]. The most well-known distribution in time–frequency power spectral analysis is WV distribution whose properties and applications have been extensively studied [2–4,6].

*Tel.: +617 5552 9175; fax: +617 5552 8065.
E-mail address: K.Le@griffith.edu.au.

0022-460X/$ - see front matter © 2005 Elsevier Ltd. All rights reserved.
doi:10.1016/j.jsv.2005.11.005

Time–frequency power spectra (time–frequency distributions) can be generalised by Cohen's [6] class which is given by the following formula:

$$P(t,\omega)=\frac{1}{4\pi^2}\int_{-\infty}^{+\infty}\int_{-\infty}^{+\infty}\int_{-\infty}^{+\infty}\underbrace{[\mathrm{e}^{-\mathrm{j}\theta(t-u)}\Phi(\theta,\tau)]}_{W(t-u,\tau)}\,\mathrm{e}^{-\mathrm{j}\tau\omega}\,R_{t,1}(t,\tau)\,\mathrm{d}u\,\mathrm{d}\tau\,\mathrm{d}\theta, \tag{1}$$

where $\Phi(\theta,\tau)$ is a kernel function, $R_{t,1}(t,\tau)=x(u+(\tau/2))x^*(u-(\tau/2))$ a local auto-correlation function, $x(\cdot)$ the input signal, t the time parameter, τ a lag parameter, $u=t+(\tau/2)$, and $W(t-u)$ the Fourier transform of $\Phi(\theta,\tau)$ which acts as a filter of $R_{t,1}(t,\tau)$. From Eq. (1), it is clear that properties of a time–frequency power spectrum are significantly dependent on the kernel function $\Phi(\theta,\tau)$. For WV time–frequency power spectrum, $\Phi(\theta,\tau)=1$ or unity kernel. Over the years, many techniques and new kernels, such as CW kernel [8] with $\Phi_{\mathrm{CW}}(\theta,\tau)=\exp(-\theta^2\tau^2/\sigma)$, multi-form tiltable exponential (MFTE) kernel [9] with

$$\Phi_{\mathrm{MFTE}}(\theta,\tau)=\exp\left\{-\pi\left[\left[\frac{\tau}{\tau_0}\right]^2\left(\left[\frac{\theta}{\theta_0}\right]^2\right)^{\alpha}+\left(\left[\frac{\tau}{\tau_0}\right]^2\right)^{\alpha}\left[\frac{\theta}{\theta_0}\right]^2+2r\left(\left[\frac{\tau\theta}{\tau_0\theta_0}\right]^{\beta}\right)^{\gamma}\right]^{2\lambda}\right\}$$

and Hy kernel [10] with $\Phi_{\mathrm{Hy}}(\theta,\tau)=\mathrm{sech}(\beta\theta\tau)$, have been proposed which possess better properties than WV kernel. A comprehensive review of available kernels can be found in Ref. [6].

Wavelet signal processing has also found many applications and has been used in conjunction with time–frequency signal processing to provide a benchmark for performance comparisons. Moreover, it has been found that there exists a link between time–frequency kernels and symmetrical wavelet functions as reported by Le and co-workers [10,11]. Time–frequency and wavelet power spectral analyses have been successfully used to study chaos, music and speech in Refs. [12–15]. Even though WV distribution is very useful and effective because it is the most simplest and energy-concentrated form of time–frequency distribution, it still suffers from a number of drawbacks. First, WV distribution may give misleading information about the input signal because WV time–frequency power spectrum is non-zero over the period in which the signal is zero (silent period). This fact has been reported in Ref. [16]. Second, other time–frequency distributions, such as CW or Hy, have been shown to be more noise robust and effective than WV distribution.

3. Properties of WV time–frequency power spectrum

Recently, Zou and Chen [1] used WV time–frequency distribution and continuous wavelet transform to study cracks in rotors with promising results. The usefulness of these techniques was also measured by studying their sensitivity with rotor stiffness, and effects of unbalance angles. The work by Zou and Chen has set up a foundation for other works on using time–frequency signal processing to study cracks in rotors. Because of the nature of cracks, rotors with cracks tend to possess non-stationary waveforms which require time–frequency analyses to process.

Theoretically, WV distribution is the most energy-concentrated distribution in Cohen's class because its kernel function is unity whose Fourier transform or weighting function $W(t-u)$ is an impulse, i.e. there is no energy smearing on the frequency plane of WV time–frequency spectrum, which can be written as

$$P(t,\omega)=\int_{-\infty}^{+\infty}x\left(t+\frac{\tau}{2}\right)x\left(t-\frac{\tau}{2}\right)\mathrm{e}^{-\mathrm{j}\tau\omega}\,\mathrm{d}\tau \tag{2}$$

or in discrete form

$$P(t,\omega)=2\sum_{\tau/2=0}^{+\infty}x\left[t+\frac{\tau}{2}\right]x\left[t-\frac{\tau}{2}\right]\mathrm{e}^{-\mathrm{j}\tau\omega} \tag{3}$$

for each pair of t and ω.

From Eqs. (2) and (3), it is clear that WV distribution is dependent on past values of the input signal which is evidenced by the pivoting of the lag parameter $\tau/2$ around the time t which causes the distribution attaining non-zero values over a zero period in the input signal $x(t)$. The normal range of $\tau/2$ can be defined as half of the duration of the input signal. However, the effective range of $\tau/2$ is dependent on the defined period of $x(t)$

as t varies, which will be demonstrated by examples. It should also be noted that on time–frequency plane of time–frequency distributions, there are cross-terms, due to cross-coupling of multi-component signals, and auto-terms, auto-coupling of multi-component signals themselves, of which the former need to be eliminated to avoid misleading information about the signals. However, it is almost impossible to remove cross-terms because there does not exist a perfect weighting function which can suppress all cross-terms and, at the same time, support all auto-terms.

The key to work out over which time period(s) WV distribution of a signal with a silent period is zero or non-zero is two-fold: first, defining the pivot point with the time origin at the beginning of the silent period; second, folding the left- and right-hand portions of the signal about the pivot point to identify any overlapped part(s). If the overlapped part(s) are non-zero, then WV distribution at that point is non-zero and vice versa. Consider an example given in Fig. 1 in which a finite-duration signal has a silent period ac.

Imagine that the time origin is at point a in Fig. 1, at which the effective swing of $\tau/2$ is from a_1 to b with a the pivot or middle point. At this instance, WV distribution is zero which truly reflects the nature of $x(t)$ which is zero. As t approaches b, the effective swing of $\tau/2$ becomes a_1 to a_{1b}, and it is clear that when t is at b, $x(t)$ over the periods of a_1a and ca_{1b} is not zero, causing $R_{1,t}(\tau)$ to be non-zero, yielding a non-zero WV distribution. The actual display of WV distribution is plotted in Fig. 2.

Consider a second example given in Fig. 3 with a longer silent period in the signal than in Example 1.

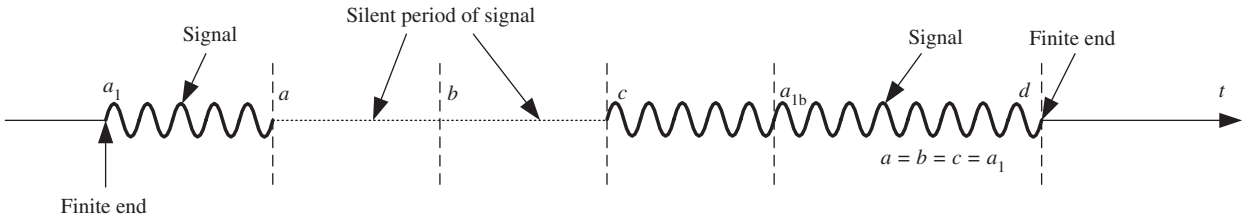

Fig. 1. Example 1—a finite input signal $x(t)$ with a silent period ac.

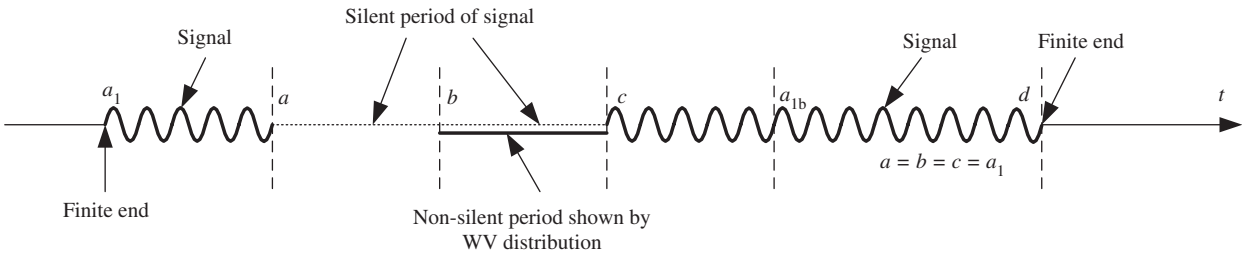

Fig. 2. A non-silent period of WV distribution over the silent period in the input signal. WV distribution is zero over the ab period which truly yields correct information about the signal.

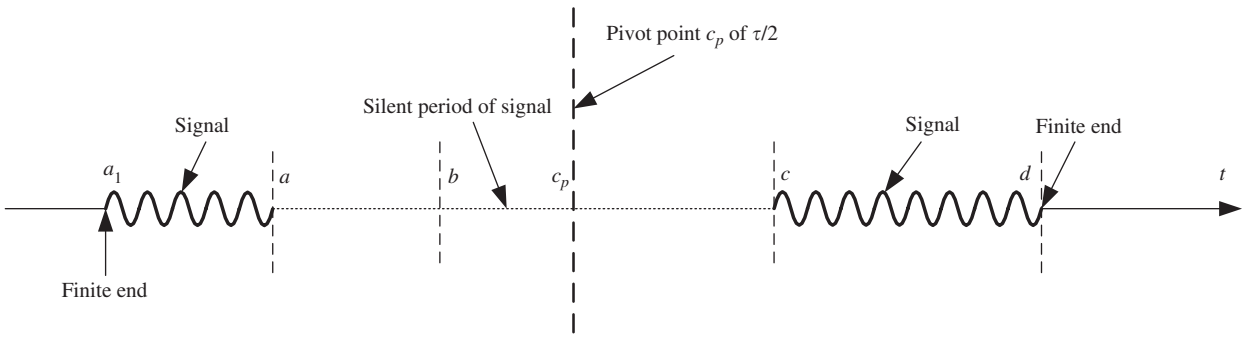

Fig. 3. Example 2—a finite input signal with a longer silent period and a pivot point c_P.

Similar to Example 1, as t reaches point b, WV distribution becomes non-zero as there is a non-zero overlapped component of the signal at points a_1 and c in Fig. 3. At the pivot point c_P of $x(t)$, WV distribution is still non-zero (because ac_P is longer than c_Pc) until t is a distance of a_1a from c_P to the right then it becomes zero again as now the overlapped component of $x(t-\tau/2)$ and $x(t+\tau/2)$ is zero. The actual display of WV distribution is plotted in Fig. 4. If $x(t)$ is infinite, then WV distribution will become non-zero for the entire period from b to c as there is always a non-zero overlapped component in the input signal.

From the above two examples, it can be said that if there are non-zero overlapped signal components over a silent period in the signal, then its WV distribution will be non-zero over the particular silent period,

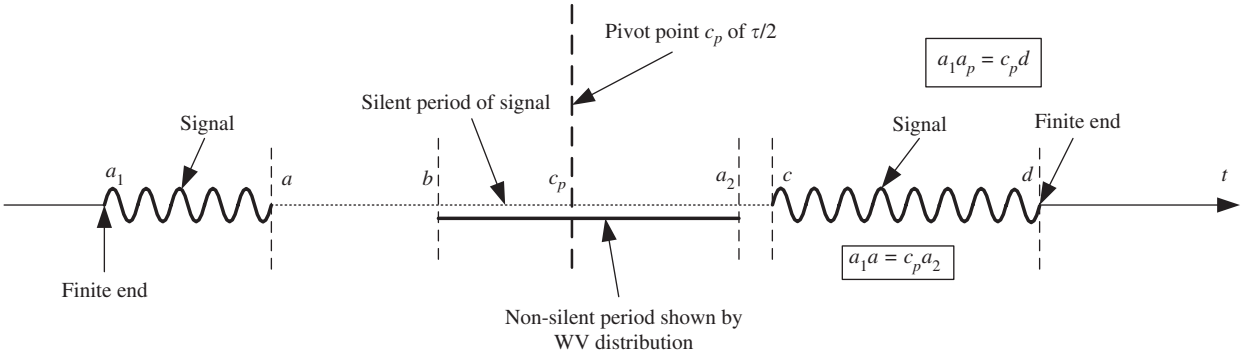

Fig. 4. A non-silent period of WV distribution of the input signal shown in Fig. 3. WV distribution is zero over the ab and a_2c periods.

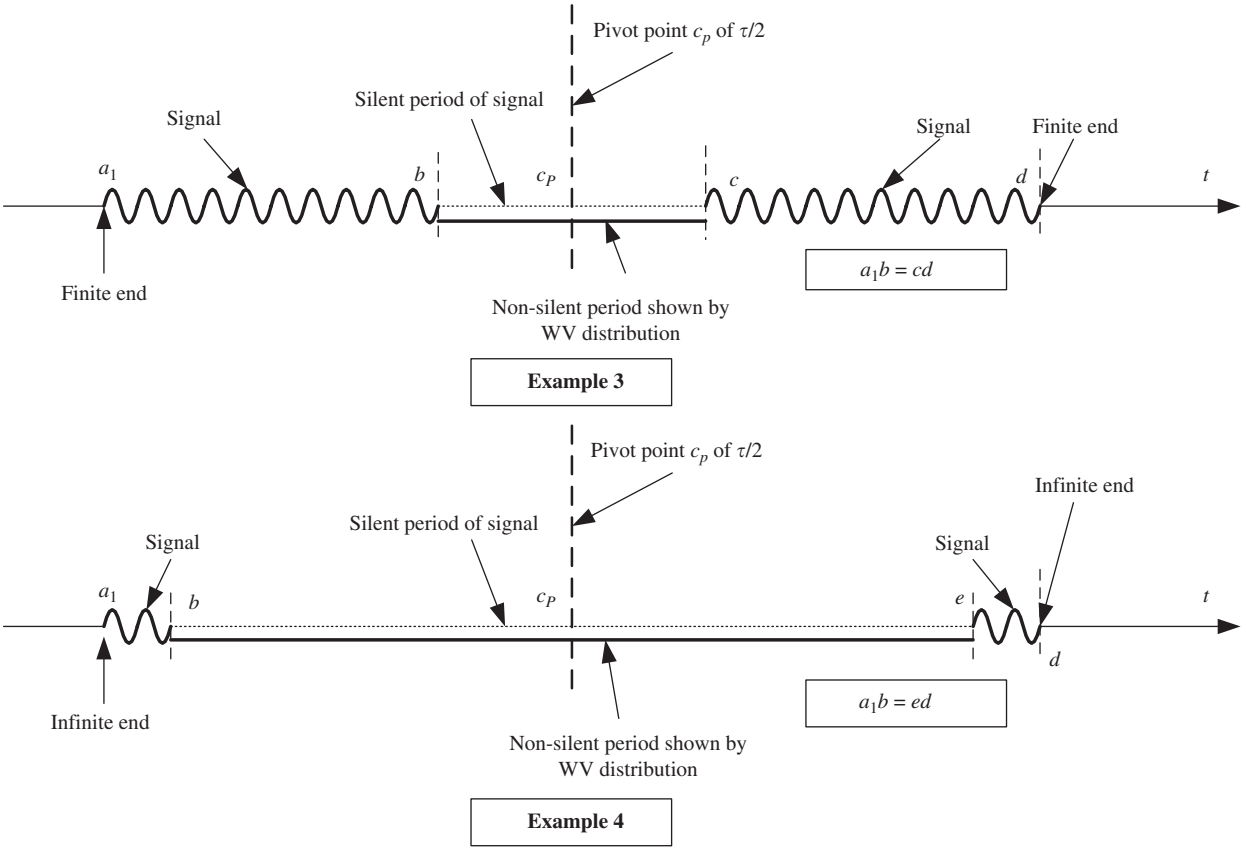

Fig. 5. Different input signals with silent periods and their corresponding WV time–frequency power spectra.

independent of the position of the time t, which yields misleading information about the signal. It should also be noted that WV distribution of a signal may be zero over part of a silent period in the signal as seen in Fig. 4. In addition, it is always true that WV time–frequency power spectra of infinite signals are non-zero over a finite silent period in the signal. Thus, to make WV time–frequency distribution more effective, infinite signals should be segmented into a number of segments, which are then processed individually. This is particularly suitable for non-stationary waveforms collected from cracked rotors. If the input signal does not consist of silent period(s) but noise, WV time–frequency distribution still suffers from its noise-spreading drawback which will be explained later in this section. The following examples further illustrate the behaviour of WV time–frequency power spectrum in different scenarios in which the input signal has a silent period (Fig. 5).

For CW and Hy distributions, cross-terms can be effectively eliminated by multiplying them with the weighting function $W(t-u)$ of which small weighting factors are allocated to cross-terms and much larger weighting factors are reserved for auto-terms. For WV kernel, since it is a unity kernel, its weighting function is an impulse which magnifies independently with identical weighting factors to every cross-term and auto-term in its time–frequency plane, yielding artefact (cross-terms) as seen in the above examples and also later in Section 5 of this paper. Thus, to make WV time–frequency distribution effective, it is crucial that "silent periods" or any salient features in the input signal must be known beforehand which makes WV distribution less practical than CW and Hy distributions for unknown signals.

Similar to the "silent period" examples shown above, if noise is now present in the input signal, then it will be spread out to other time and frequency bins on the time–frequency plane of WV distribution which makes it sensitive to noise, and therefore not noise robust [16] as illustrated by the following examples given in Figs. 6 and 7. A more detailed study on noise in time–frequency power spectra can be found in Refs. [7,10].

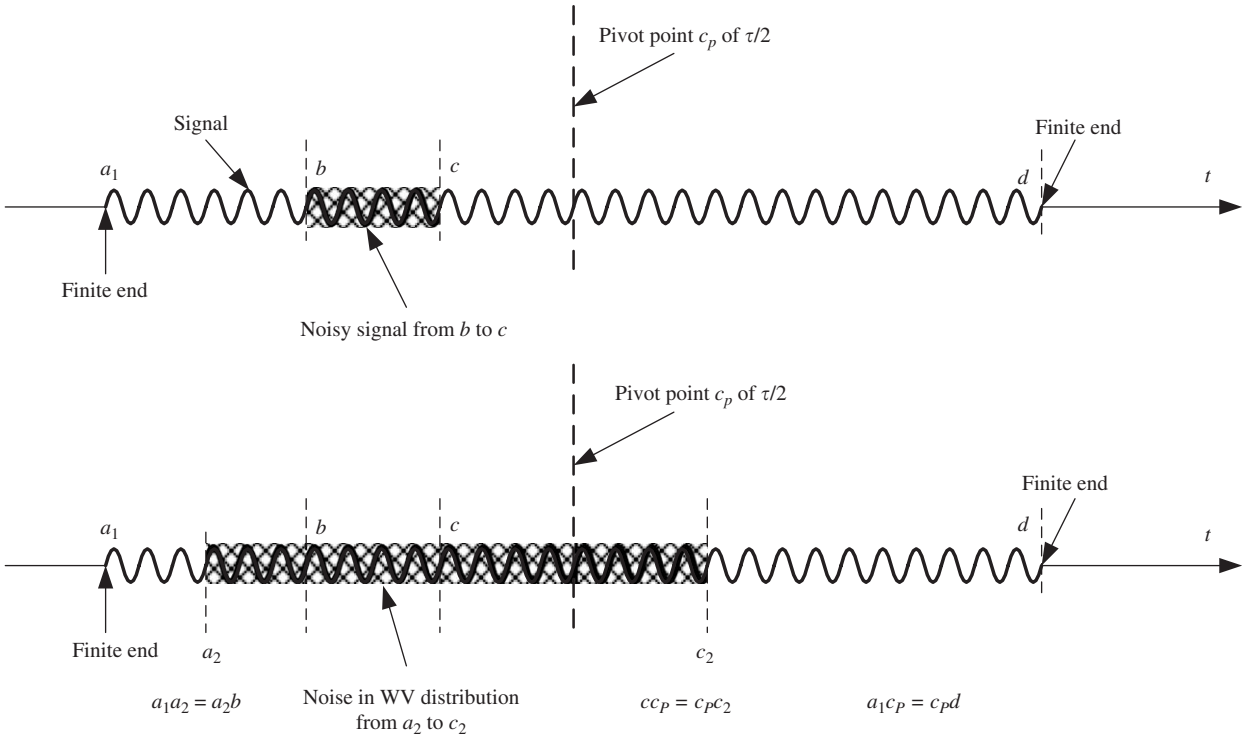

Fig. 6. A finite signal contaminated with noise and its WV distribution which also spreads the noise to other time locations. The noisy period in WV distribution is worked out using the same principle applied to the previous four examples.

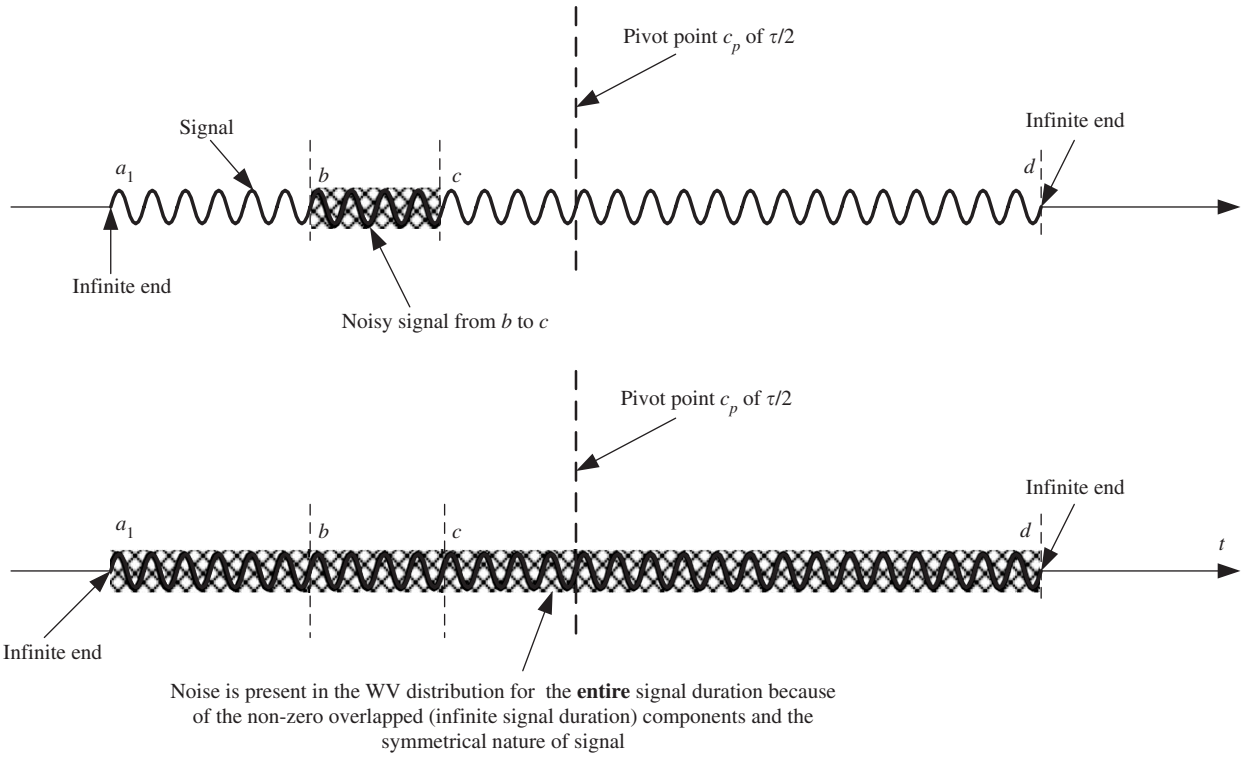

Fig. 7. An infinite signal contaminated with noise and its WV time–frequency spectrum which spreads the noise over the entire signal length.

4. Relationship between time–frequency kernels and symmetrical wavelets

A relationship between time–frequency kernels and symmetrical wavelets was reported by Le et al. [17], in which symmetrical wavelet can be generated from their time–frequency kernels counterpart by taking the kernels' second-order derivatives. One typical example is the Mexican-hat wavelet which is the second-order derivative of the Gaussian kernel. The Hy wavelet, second-order derivative of Hy kernel, was also proposed and used to study music and speech in Ref. [12]. According to the second-order derivative rule which has been successfully applied to CW and Hy kernels, a WV wavelet does not exist since its kernel is unity. Mathematically, CW and Hy wavelets are given in the time domain as

$$\psi_{\mathrm{Hy}}(t) = -\beta^2[\mathrm{sech}(\beta t)]\{1 - 2[\mathrm{sech}(\beta t)]^2\}, \tag{4}$$

$$\psi_{\mathrm{CW}}(t) = (2/\sigma)\exp(-t^2/\sigma)(-1 + 2t^2/\sigma), \tag{5}$$

which are normalised and plotted in Fig. 8.

In the frequency domain, the Fourier transform of the wavelets are given as

$$\hat{\psi}_{\mathrm{Hy}}(\omega) = \frac{\pi\omega^2}{\beta}\,\mathrm{sech}(\pi\omega/2\beta), \tag{6}$$

$$\hat{\psi}_{\mathrm{CW}}(\omega) = \sqrt{\pi\sigma}\,\omega^2\exp(\pi\omega^2/4), \tag{7}$$

which are, respectively, plotted in Figs. 9 and 10.

The existence of Hy and CW wavelets are validated by their mathematical expressions given by Eqs. (4)–(7). The CW wavelet is also known as Mexican-hat wavelet or Laplacian of Gaussian which has been widely accepted and used in many fields of science [18]. The relationship between time–frequency kernels and

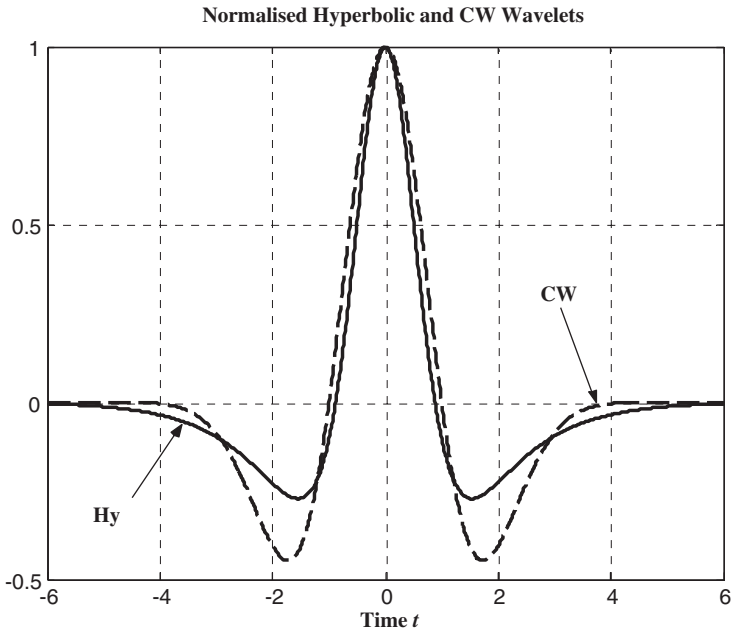

Fig. 8. Time-domain plots of the Hy and CW wavelets, for $\beta = 1$ and $\sigma = 2$.

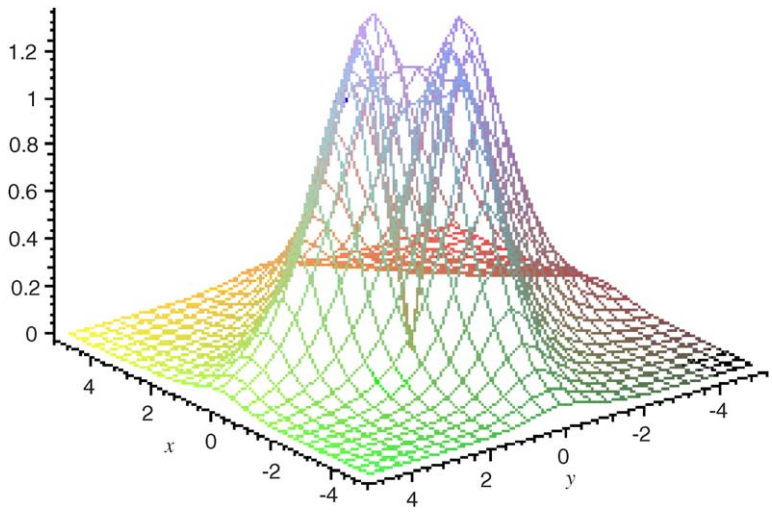

Fig. 9. Magnitude of the 2-D frequency response of the Hy wavelet, for $\beta = 1$.

wavelets diversifies time–frequency spectral analyses and continuous wavelet power spectral analyses, i.e. new time–frequency distributions can be found from new and existing wavelets and vice versa. With a variety of time–frequency distributions, cracks in rotors can be more effectively studied. More work on using wavelet power spectral analyses is currently in progress and will be reported in future publications.

5. WV, CW and Hy time–frequency power spectral analyses for feature extraction

This section aims to graphically illustrate the effectiveness of CW and Hy distributions over WV distribution, thus makes them suitable candidates for crack detection in rotors. Section 5.1 graphically

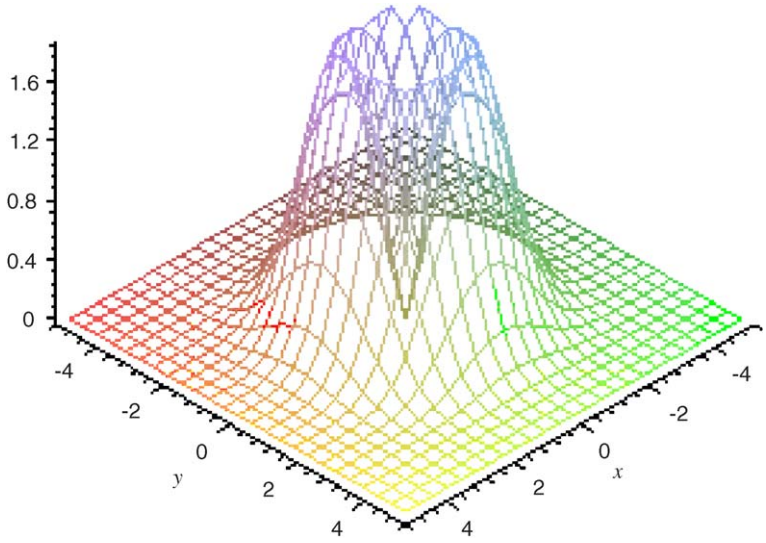

Fig. 10. 2-D frequency response magnitude of the CW wavelet, for $\sigma = 2$.

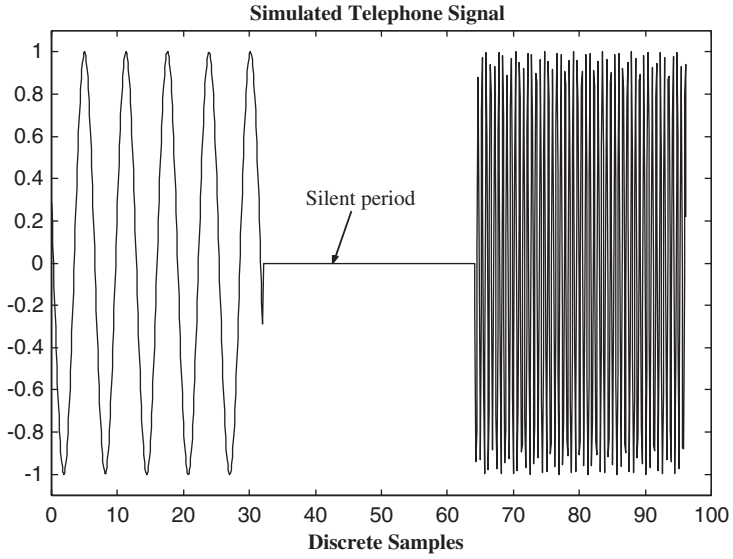

Fig. 11. A simulated speech signal with a silent period from the 32nd to 64th sample.

illustrates that WV distribution could not detect a silent period which is common in speech signals. Section 5.2 shows that Hy and CW distributions are more effective in terms of suppressing cross-terms and detecting main harmonics in a cracked-rotor waveform.

5.1. Detection of a silent period in a speech signal

Consider the following simulated speech signal given in Fig. 11. The signal consists of two harmonics which are linked by a silent period. WV, CW and Hy time–frequency power spectra are plotted in Figs. 12–14, respectively.

As can be seen in Fig. 12, it is clear that WV time–frequency power spectrum is non-zero over the time period between the 32nd and 64th sample which provides misleading information about the signal. Over the

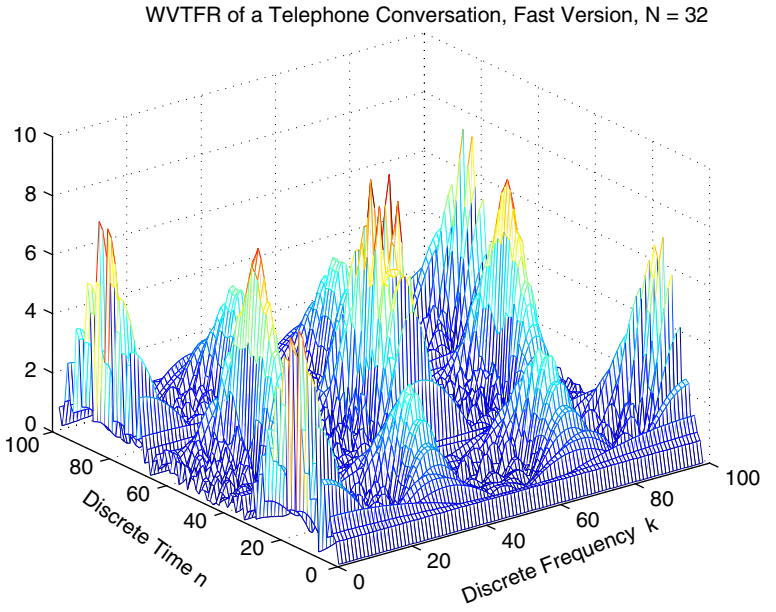

Fig. 12. WV time–frequency power spectrum of the speech signal given in Fig. 11.

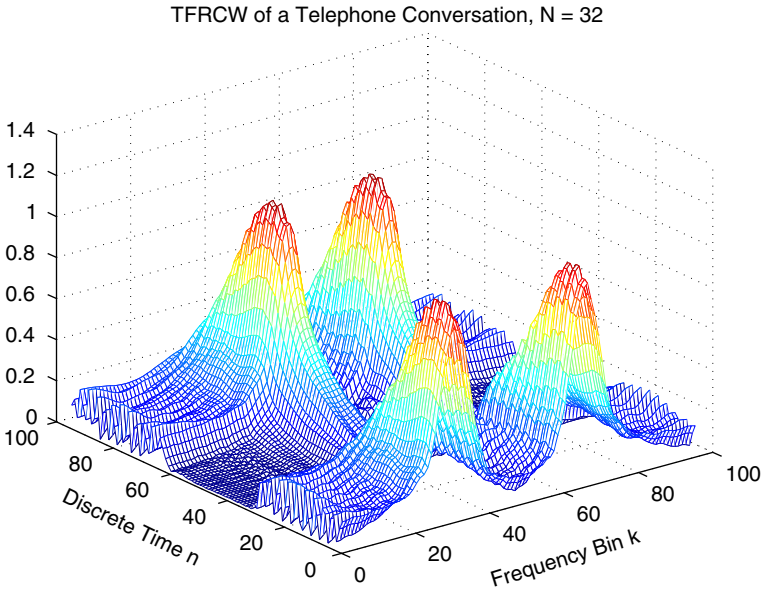

Fig. 13. CW time–frequency power spectrum of the speech signal given in Fig. 11.

same time period, CW and Hy time–frequency power spectra effectively detect the silent period in the input signal, and the latter provides a better result. The main reason why CW and Hy kernels can outperform WV kernel is because their kernels are not unity which provides better cross-term suppression and noise robustness [10,19]. From this point of view, these time–frequency distributions can be employed to study cracks in rotors more effectively than using WV distribution. Even though the work by Zou and Chen [1] has formed a solid foundation of introducing time–frequency power spectral analyses to detect cracks in rotors, it would be more complete if other kernels in Cohen's class, such as CW and Hy, be utilised so that more salient features in the input signal from cracked and uncracked rotors can be effectively identified.

5.2. Detection of cracks in rotors

The dynamic equation of a cracked rotor is given as [1]

$$\begin{bmatrix} m & 0 \\ 0 & m \end{bmatrix} \begin{pmatrix} \ddot{x} \\ \ddot{y} \end{pmatrix} + \begin{bmatrix} c & 0 \\ 0 & c \end{bmatrix} \begin{pmatrix} \dot{x} \\ \dot{y} \end{pmatrix} + \begin{bmatrix} k_x & k_{xy} \\ k_{yx} & k_y \end{bmatrix} \begin{pmatrix} x \\ y \end{pmatrix} = \begin{pmatrix} F_x \\ F_y \end{pmatrix} + \begin{pmatrix} mg \\ 0 \end{pmatrix}, \tag{8}$$

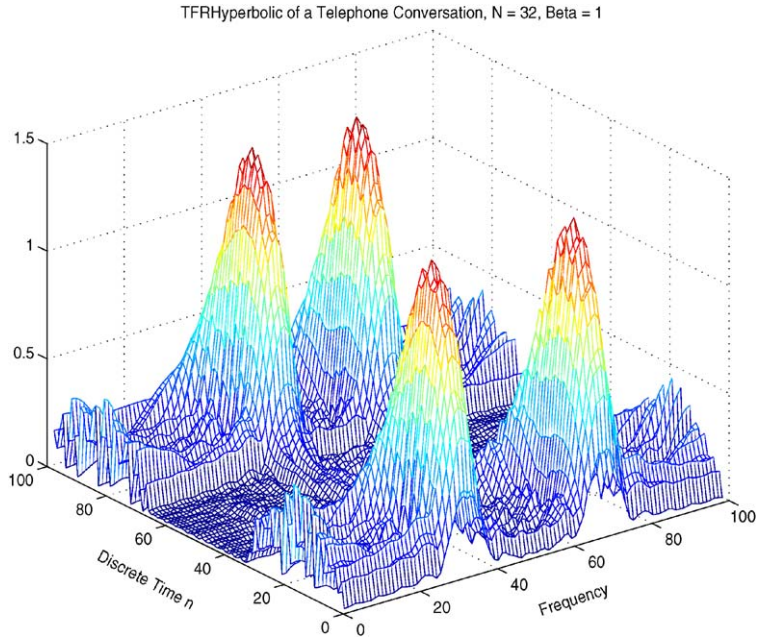

Fig. 14. Hyperbolic time–frequency power spectrum of the speech signal given in Fig. 11.

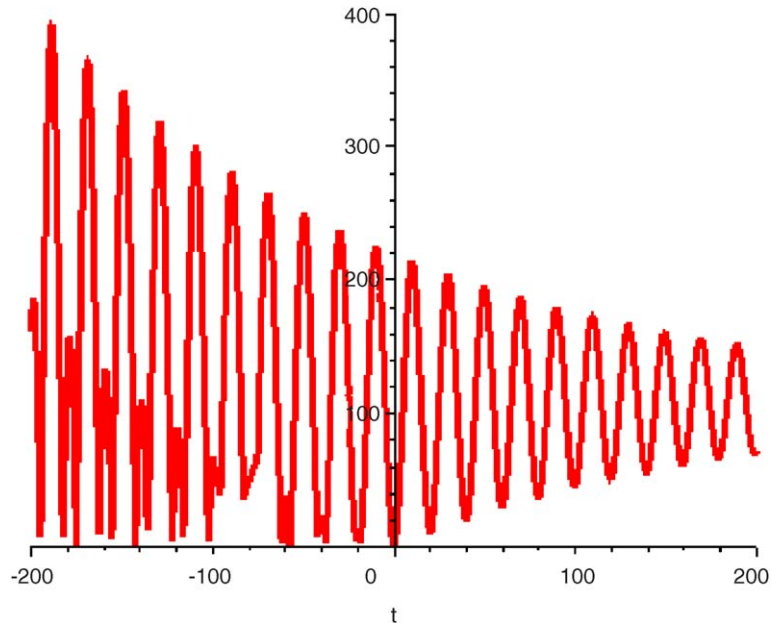

Fig. 15. A time-domain waveform of a cracked rotor under arbitrary initial conditions.

where m is the disc mass, c the damping coefficient; k_x, k_y, k_{xy} and k_{yx} stiffness coefficients; and F_x and F_y excitation forces. By solving for $x(t)$, one obtains an equation of motion of the cracked rotor with respect to t as shown in Fig. 15 under arbitrary conditions of $F = 1\,\mathrm{N}$, $m = 1\,\mathrm{kg}$, $g{\sim}10\,\mathrm{m/s^2}$, $c = 0.01$ and $k = 0.1\,\mathrm{N/m}$.

Figs. 16, 17 and 18, respectively, plot the Hy, CW and WV time–frequency distributions of the cracked-rotor signal shown in Fig. 15. From Figs. 16 and 17, it is clear that the location of the signal's main harmonic is located over the low frequency range of $f < 50\,\mathrm{Hz}$. From Fig. 18, WV distribution can locate the main harmonic of the waveform but it cannot identify the signal's fine sub-harmonic as compared to Figs. 16 and 17.

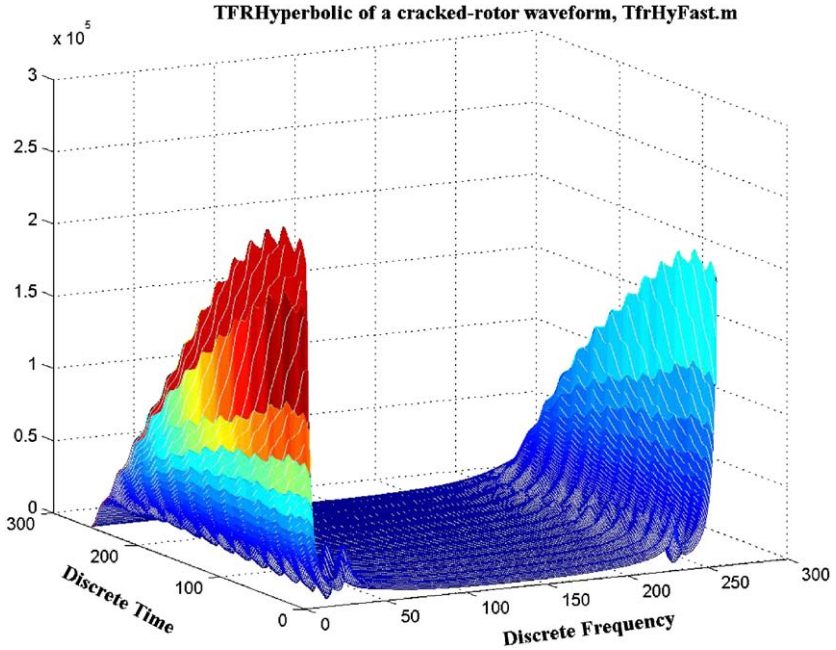

Fig. 16. Hy time–frequency power spectrum of the cracked-rotor signal shown in Fig. 15.

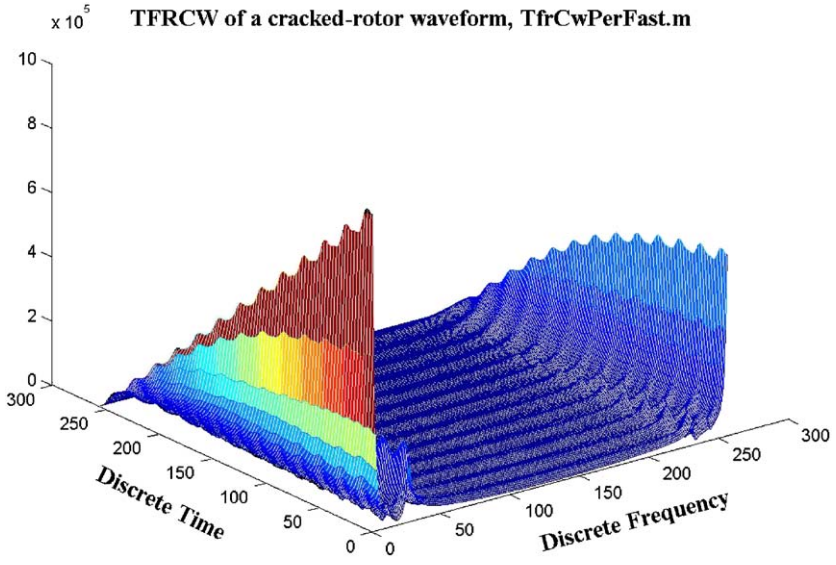

Fig. 17. CW time–frequency power spectrum of the cracked-rotor signal shown in Fig. 15.

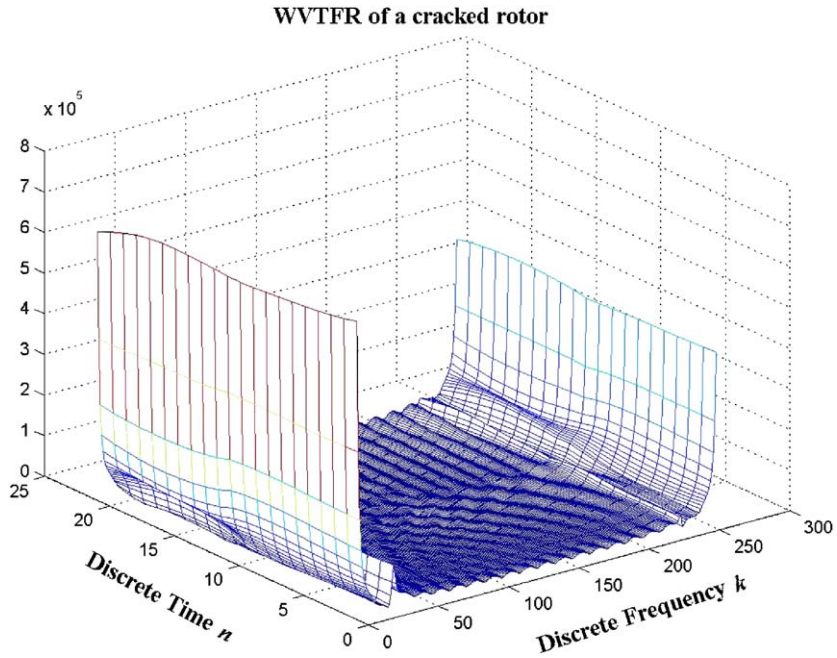

Fig. 18. WV time–frequency power spectrum of a cracked-rotor signal shown in Fig. 15.

In addition, since cross-terms are not completely suppressed by WV kernel, over the approximate frequency range of $50 \leqslant f \leqslant 200$ Hz, they are still present and are much larger than Hy and CW cross-terms shown in Figs. 16 and 17. It is, thus, evident that the Hy and CW time–frequency distributions can be considered as effective tools for crack detection in rotors. It should also be noted that the Hy time–frequency distribution is cleaner than CW distribution as less cross-terms are present over the frequency range of $50 \leqslant f \leqslant 200$ Hz. Further detailed work on crack detection in rotors under different conditions is currently in progress and will be reported in separate publications.

6. Conclusions

This correspondence has shown that WV time–frequency power spectrum (distribution) could provide misleading information about signals with silent periods due to the presence of cross-terms. If the input signal consists of noise, its WV time–frequency power spectrum also spreads the noise to other time and frequency locations. Even though WV distribution is useful because of its simplicity, great care should be taken when implementing it.

CW and Hy time–frequency power spectral analyses have been successfully used for crack detection in rotors because of their ability to more effectively suppress cross-terms, support auto-terms and possessing better noise robustness than WV distribution. Detailed work on using the Hy and CW wavelet power spectral analyses for crack detection in motors is currently in progress. More detailed work on using Hy and CW time–frequency power spectral analyses under different initial conditions is also in progress.

References

[1] J. Zou, J. Chen, A comparative study on time–frequency feature of cracked rotor by Wigner–Ville distribution and wavelet transform, *Journal of Sound and Vibration* 276 (1–2) (2004) 1–11.

[2] T.A.C.M. Claasen, W.F.G. Mecklenbrauker, The Wigner distribution—a tool of time–frequency signal analysis—part I: discrete-time signals, *Philips Journal of Research* 35 (3) (1980) 217–250.

[3] T.A.C.M. Claasen, W.F.G. Mecklenbrauker, The Wigner distribution—a tool for time–frequency signal analysis—part III: relations with other time–frequency signal transformations, *Philips Journal of Research* 35 (6) (1980) 372–389.
[4] T.A.C.M. Claasen, W.F.G. Mecklenbrauker, The Wigner distribution—a tool for time–frequency signal analysis—part II: continuous-time signals, *Philips Journal of Research* 35 (4–5) (1980) 276–300.
[5] L. Cohen, *Time–frequency Analysis*, Prentice-Hall, Englewood Cliffs, NJ, New York, 1995 (pp. 136–289).
[6] L. Cohen, Time–frequency distribution—a review, *IEEE Proceedings* 77 (7) (1989) 941–981.
[7] L. Stankovic, V. Ivanovic, Further results on the minimum variance time–frequency distribution kernels, *IEEE Transactions on Signal Processing* 45 (6) (1997) 1650–1655.
[8] H.I. Choi, W.J. Williams, Improved time–frequency representation of multi-component signals using exponential kernels, *IEEE Transactions on Signal Processing* 37 (6) (1989) 862–871.
[9] A.H. Costa, G.F. Boudreaux-Bartels, Design of time–frequency representation using a multiform, tiltable exponential kernel, *IEEE Transactions on Signal Processing* 43 (10) (1995) 2283–2301.
[10] K.N. Le, K.P. Dabke, G.K. Egan, Hyperbolic kernel for time–frequency power spectrum, *Optical Engineering* 42 (8) (2003) 2400–2415.
[11] K.N. Le, High-order symmetrical wavelets, submitted for publication.
[12] K.N. Le, K.P. Dabke, G.K. Egan, Hyperbolic wavelet power spectra of non-stationary signals, *Optical Engineering* 42 (10) (2003) 3017–3037.
[13] B.P. van Milligen, C. Hidalgo, E. Sanchez, Nonlinear phenomena and intermittency in plasma and turbulence, *Physical Review Letters* 74 (3) (1995) 395–398.
[14] B.P. van Milligen, et al., Wavelet bicoherence: a new turbulence analysis tool, *Physics of Plasmas* 2 (8) (1995) 3017–3032.
[15] M. Farge, et al., Wavelets and turbulence, *Proceedings of the IEEE* 84 (4) (1996) 639–669.
[16] L. Cohen, On a fundamental property of the Wigner distribution, *IEEE Transactions on Acoustics, Speech, and Signal Processing* ASSP-35 (4) (1987) 559–561.
[17] K.N. Le, K.P. Dabke, G.K. Egan, Hyperbolic wavelet family, *Review of Scientific Instruments* 75 (11) (2004) 4678–4693.
[18] I. Daubechies, The wavelet transform, time–frequency localization and signal analysis, *IEEE Transactions on Information Theory* 36 (5) (1990) 961–1005.
[19] K.N. Le, K.P. Dabke, G.K. Egan, On mathematical derivation of auto-term function, signal-to-noise ratios of Choi–Williams, first- and *n*th-order hyperbolic kernels, *Digital Signal Processing: A Review Journal* 16 (1) (2006) 84–104.